



Contents lists available at ScienceDirect

Resources, Conservation & Recycling

journal homepage: www.elsevier.com/locate/resconrec

Full length article

Characterisation of excavated landfill waste fractions to evaluate the energy recovery potential using Py-GC/MS and ICP techniques

Katarzyna Jagodzińska^{a,*}, Cristina Garcia-Lopez^b, Weihong Yang^a, Pär Göran Jönsson^a, Thomas Pretz^b, Karoline Raulf^b

^a KTH Royal Institute of Technology, Department of Material Sciences and Engineering, Brinellvägen 23, Stockholm, Sweden

^b RWTH University Aachen, Department of Processing and Recycling, Aachen, 5206, Germany



ARTICLE INFO

Keywords:

Enhanced landfill mining
Waste management
Circular economy
TG, pyrolysis

ABSTRACT

Fuelled by further planet degradation concerns, the circular economy concept spreads worldwide, incorporating the need for the closing of material loops. This can be done not only by waste prevention and recycling but also by excavating old landfill sites. In line with this need, the Enhanced Landfill Mining concept was developed, which covers mining of old landfills combined with material and energy recovery from the excavated material. Site-specific investigations of excavated material are required because the way of excavated material utilisation has to be individually tailored to the material features. In this article, the valorisation options for the excavated waste from the old part of the landfill located in Mont-Saint-Guibert (Belgium) are preliminarily assessed. Seven separated waste fractions were analysed regarding their thermal decomposition pattern (TGA), pyrolysis potential (Py-GC/MS), and elemental composition (ICP-OES). Most of the analysed fractions are characterised by a highly heterogeneous composition, which excludes their primary or secondary recycling. The fractions are also characterised by high calorific value, which indicates the potential for thermochemical utilisation (i.e., pyrolysis). The presence of a significant amount of heavy metals (especially Hg and Pb) and chlorine may, however, pose a considerable risk of the contamination of pyrolysis products. It may require costly washing of the feed-stock prior to the utilisation or cleaning of the process products prior to their use. Therefore, in order to limit additional costs, collective pyrolysis of all fractions seems to be a feasible way of their utilisation.

1. Introduction

Unquestionably, waste generation has been an inevitable consequence of economic activities over the centuries. Swift industrialisation, urbanisation and, consequently, population growth led to the accumulation of residues and their disposal in the form of landfills. Those landfills pose a considerable risk of groundwater and soil pollution (Hernández Parrodi et al., 2019b), for instance, caused by asbestos Brand and Spencer (2018) or microplastics (He et al., 2019). However, at the time when Earth's climate is on a slope of irreversible and calamitous change, the action against further planet degradation is a necessity. In response to this threat, the circular economy concept spreads worldwide, addressing the need for waste prevention and recycling (European Commission, 2020; Ghosh et al., 2020; Pesce et al., 2020).

Closing of material loops by following the circular economy approach can be done not only by recycling of pre- and post-consumer

residues but also by mining old landfill sites (Jones et al., 2013). Landfill mining in its early form, however, was primarily motivated by the end of landfill's operational life or the need of land reclamation (Hogland et al., 2004; Johansson et al., 2012). Furthermore, the incineration of excavated material was seen as the most feasible way of their utilisation (Quaghebeur et al., 2013; Zhou et al., 2014). Nevertheless, as a result of the progressive implementation of the circular economy concept, the transformation of the existing landfills into the source of secondary materials and energy have recently gained public attention (Esguerra et al., 2019). Consequently, landfill mining evolved into the so-called Enhanced Landfill Mining (ELFM). The ELFM includes excavation of old landfills combined with the material recovery and the subsequent formation of refuse-derived fuel (RDF) from non-recyclable plastics, textiles, wood, and paper while fulfilling rigorous ecological and social criteria (Jones et al., 2013).

The excavated waste features vary according to, among others, their type (i.e., industrial, construction and demolition, hazardous, or

* Corresponding author.

E-mail address: kjag@kth.se (K. Jagodzińska).

<https://doi.org/10.1016/j.resconrec.2021.105446>

Received 26 August 2020; Received in revised form 4 November 2020; Accepted 18 January 2021

Available online 29 January 2021

0921-3449/© 2021 The Author(s). Published by Elsevier B.V. This is an open access article under the CC BY license (<http://creativecommons.org/licenses/by/4.0/>).

municipal solid waste), landfill age or its geographical location (Kaarinen et al., 2013; Lokahita et al., 2019; Singh and Chandel, 2019; Ximenes et al., 2018). Despite this, some congruity between them can be listed, such as the relatively high contents of heavy metals and low calorific value due to the considerable content of a soil-like fraction. Overall, however, the site-specific investigations are always essential (Krook et al., 2012), and the technologies for the excavated material utilisation have to be individually tailored to the material features.

Finding a feasible way to valorise the excavated material may be arduous due to, inter alia, the aforementioned significant content of soil-like material. This material could be used as soil fertiliser, construction material or top-soil cover for operating landfills, although with prior treatment reducing its biological activity and possibly its heavy metal content (Mönkäre et al., 2019). (Mönkäre et al., 2019, 2017, 2016) attempted to answer the question on the feasibility of the biological treatment of such excavated soil-like material, based on available technologies for waste and contaminated soil management. The proposed solution is technically feasible, yet economically ambiguous due to a wide range of unknowns, especially connected with the income from treated material (i.e., its price as, for example, construction material). This uncertainty can only be addressed individually for a particular case, taking into account the excavated material composition, contamination and the current social and legal context (i.e., landfill tax).

Previous investigations also concentrated on the potential valorisation of the excavated paper, wood, textiles (Quaghebeur et al., 2013; Wolfsberger et al., 2015), and plastics (Zhou et al., 2014). Due to their heterogeneous composition and high contamination level, incineration is currently considered as the most suitable method of their utilisation. Nonetheless, the new Circular Economy Action Plan for a cleaner and more competitive Europe European Commission (2020) encourages the stimulation of the circular economy by implementing several economic instruments such as landfill and waste incineration taxes. This fuels attention for other available waste-to-energy technologies, such as gasification or pyrolysis.

Pyrolysis and gasification are considered as competing technologies (Salaudeen et al., 2018). Both of them, however, offer complementary ways of excavated waste valorisation, especially for non-recyclable and non-compostable fractions (Ciuta et al., 2017a, 2017b). Therefore, research on both of them is advantageous for the Enhanced Landfill Mining (ELFM) which, as an emerging concept, faces a deficit in generic knowledge on it as a whole and, consequently, lacks systematic understanding of its economic performance (Laner et al., 2019).

Several studies have been performed on excavated waste gasification. (Agon et al., 2016) investigated plasma gasification with seven different gasifying agents, whereas (Zaini et al., 2019, 2017) studied kinetics and char reactivity in steam and steam/air gasification of refuse-derived fuel (RDF) formed from excavated waste. Additionally, (Zaini et al., 2020) studied excavated waste and biochar co-gasification in a steam atmosphere with various waste/biochar ratios at different temperatures. On the contrary, a thorough search of relevant literature yielded only two articles on the excavated waste pyrolysis. (Bosmans et al., 2014) performed a thermogravimetric analysis of excavated waste pyrolysis, whereas (Breyer et al., 2017) studied the pyrolysis of excavated plastics and used lubrication oils to produce an alternative fuel suitable for cement kilns. The limited number and narrow scope of previous studies on excavated waste pyrolysis show the need for more research on this matter as identified also by (Canopoli et al., 2020, 2018).

As stated above, the way of excavated material utilisation has to be individually tailored to the material features. Therefore, the main objective of this investigation is the characterisation of the excavated waste fractions individually as the preliminary assessment of their further applications. Given the above knowledge gap on the pyrolysis of excavated waste, this study presents an assessment of the analysed fractions' pyrolysis potential. For this purpose, thermogravimetric analysis was combined with analytical pyrolysis (Py-GC/MS) to

investigate the fractions' thermal degradation pattern and their material composition qualitatively. Several fractions were taken into account, namely: two plastic fractions, wood, paper, textiles and the remaining unclassified fraction (further referred to as the *rest* fraction). Additionally, the analysis was extended with the determination of the fractions' elemental compositions, including the heavy metal contents, broadening the perspective on their possible application. To the best of our knowledge, this is the first characterisation of excavated waste using Py-GC/MS technique presented in the open literature.

2. Material and methods

2.1. Feedstock preparation

The material used within the study was excavated from the oldest part of a landfill located in Mont-Saint-Guibert (Belgium). Approximately 5.7 million m³ of construction and demolition waste, municipal solid waste, and non-hazardous industrial waste were disposed at the landfill between 1958 and 1985 (Greisch, 2002; Hernández Parrodi et al., 2019a), from which approximately 130 m³ were excavated. Afterwards, the material was directly processed with a ballistic separator "STT6000 Stadler Anlagenbau GmbH" with two sieves, 200 mm and 90 mm. In total, 374 tonnes of landfill waste were excavated and mechanically processed in September 2017. The flowchart of this process and the photographs of the separated fractions can be found in Fig. A1-2 in the Supplementary material, and the detailed description of the excavation and sorting process can be found in (Garcia Lopez et al., 2019).

Initially, the excavated material was ballistically separated into three material flows, according to their shape, density, and particle size. One of the obtained flows (under-screen material) had a particle size < 200 mm, and it was further processed with a 90 mm sieve and divided into three subfractions (3D 200–90 mm, 2D 200–90 mm and <90 mm). One of them, the so-called 2D subfraction (i.e., relatively light, soft particles), was subjected to further investigations within this study due to its highest potential for energy use (i.e., high calorific value). This subfraction was further processed by drying and manual sorting into ten separate fractions.

2.2. Feedstock properties

The aforementioned 2D subfraction (200–90 mm) was further investigated within this study. The feedstock was collected according to the German guideline for physical, chemical and biological testing in connection with the recovery/disposal of waste (LAGA PN 98). Subsequently, the collected sample was subjected to drying (initial moisture content was 32 wt%), which enabled a manual sorting of the sample into ten separate fractions, namely: *2D plastic*, *3D plastic*, *ferrous metals*, *fines* (< 20 mm), *inert*, *paper*, *rest*, *textiles* and *wood* fraction. The feedstock was dominated by the *2D plastic*, *fines* and *rest* fractions, which represented 37wt%, 31wt% and 10wt%, respectively. The exact composition of the 2D subfraction can be found in Table A1 in the Supplementary material. Three fractions (*ferrous metals*, *inert* and *non-ferrous metals*) were excluded from this study due to their low energy potentials.

The distinguished material fractions belong to general categories and do not have specified compositions, i.e. the *wood* fraction consists of all types of wood. Similarly, all kinds of carton and cardboard can be found in the *paper* fraction. The *2D plastic* fraction contains primarily thin foil and plastic bags, whereas the *3D plastic* fraction is mainly made of thick and hard plastic debris. The *textiles* fraction likely consists predominantly of synthetic fibres since natural materials (e.g., cotton) are more prone to degradation (Arshad and Mujahid (2011)). The *inert* fraction contains mostly ceramic and mineral fractions; so does the *fines* fraction with an ash content of approx. 74 %. The remaining part of the material (further referred to as the *rest* fraction) is a mixture of rubber, foam, hazardous wastes like sanitary material, and other unidentified

components.

The fractions were analysed in terms of their ash contents, gross calorific values, and elemental composition. Before the analysis, preparation of the samples was necessary to ensure their homogeneity and, consequently, the repeatability of the results. Several types of mills (hammer mills, disc mills and cutting mills) were used to reduce the samples' particle size to values below 1 mm. The gross calorific value was determined following the CEN/TS 16023:2013 standard, whereas the ash content was determined following the DIN 51719 standard. The samples elemental composition was determined following several standards – C, H, N following the German DIN 51732 standard, whereas the S content was determined following the DIN 51724-1:2019-10 standard. An external laboratory (Horn&Co. Analytics GmbH, Aachen, Germany) determined the Ag, Al, As, B, Ba, Be, Bi, Ca, Cd, Co, Cr, Cu, Fe, Ga, In, K, Li, Mg, Mn, Mo, Na, Nb, Ni, P, Pb, Sb, Se, Si, Sn, Sr, Ta, Te, Th, Ti, V, W, Zn, Zr contents using the ICP-OES technique, following the EN ISO 11885 standard. The laboratory also determined the Cl content following the DIN ISO 15597 standard and Hg content following the DIN EN ISO 12846 and DIN EN 1483 standards.

2.3. Thermogravimetric analysis

Thermogravimetric studies (STA 449 F1 Jupiter, NETZSCH) were performed to determine the pyrolysis temperature for each analysed fraction (2D plastic, 3D plastic, fines, paper, rest, textiles, wood). The determinations were performed for the samples with the particle size below 3 mm. The inert atmosphere was ensured by using the nitrogen flow of 50 ml/min. The sample mass varied between 100 mg and 200 mg. The TG procedure was as follows: heating at 5 °C/min to 300 °C, holding at 300 °C for 5 min, then heating at 10 °C/min to 850 °C, and finally holding at 850 °C for 10 min.

2.4. Analytics pyrolysis (Py-GC/MS)

Each material fraction (2D plastic, 3D plastic, paper, rest, textiles, wood) was analysed using a Pyrolysis-GC/MS technique (Py-GC/MS). The fines fraction was excluded from the analysis due to its low degradability. Two different degradation patterns characterise the fractions. The one-step degradation is represented by the single peak in a DTG profile and occurs for the majority of the analysed fractions (2D plastic, paper, textile, and wood). On the contrary, the two-step degradation, represented by two peaks in the DTG profile, occurred for 3D plastic and the so-called rest fraction. For that reason, the 3D plastic and rest fractions pyrolysis was performed at two temperatures to distinguish the products formed at different degradation stages.

Prior to the tests, the reduction of the fractions' particle sizes was necessary to improve the samples' homogeneity and, consequently, the repeatability of the tests. The fractions were ground to the particle size below 0.71 mm, and subsequently, the representative samples were formed by quartering.

Pyrolysis was performed in a filament pulse pyrolyser (Pyrola® 2000, Pyrol AB) coupled with the GC/MS (Agilent 7890A/Agilent 5975C). Each sample was analysed at least five times to ensure the

certain repeatability of the results. The DB-1701 column (30 m × 0.25 mm × 0.25 µm, Agilent) was used for the chromatographic separation. The mass of the pyrolysed sample varied between 0.75 mg to 1.7 mg, depending on its density. The filament heating time was 8 ms, which ensured so-called flash pyrolysis with a rapid heating rate in the range of 12,500 to 40,625 °C/s, depending on the initial temperature of the pyrolyser and the final pyrolysis temperature.

The pyrolysis temperatures were chosen based on the DTG degradation profiles for each fraction. Thus, 500 °C was selected for all the fractions as the temperature of the complete thermal decomposition, and 300 °C as the second temperature of the 3D plastic and rest pyrolysis. However, due to the variations of the filament thermal resistances and the sample masses, the set values of the pyrolysis temperature varied by ± 14 °C. The exact pyrolysis temperatures for each sample are shown in Table 1.

Two temperatures of the pyrolyser chamber were used within the study, namely 175 °C and 200 °C. An insufficient chamber temperature may promote pyrovolpours condensation before reaching the GC interface, whereas a too high temperature may result in a partial decomposition of the sample before its actual pyrolysis. For that reason, based on the DTG decomposition profiles, 200 °C was chosen for the 2D plastic fraction. However, 175 °C was selected for the 3D plastic, paper, textiles, and wood fractions, since their decompositions start at temperatures close to 200 °C.

According to (González Martínez et al., 2019), the length of the pyrolysis process has a considerable impact on the amount and type of pyrovolpours produced. Therefore, sequential pyrolysis was performed to determine the process duration for the analysed fractions, following the methodology reported by (Kleen et al., 2003; Selsbo et al., 1997). The determined pyrolysis times were 6 s and 18 s at 500 °C and 300 °C, respectively.

The GC/MS programme was adjusted individually for each sample, as it is shown in Tab. 1. The MS source and quadrupole temperatures were 230 °C and 150 °C, respectively. Samples were introduced to the GC injector at 280 °C, with a split ratio of 5:1 and the He flow of 1 ml/min. The chromatograms were qualitatively analysed using NIST-11 library, and subsequently, this analysis was manually verified. The GC/MS results are shown in the form of weight-normalised area% to enable identification of trends. The weigh-normalisation was done by dividing the peak area by the sample weight from each experiment.

3. Results and discussion

3.1. TG and Py-GC/MS analyses

Seven excavated waste fractions were subjected to the thermogravimetric analysis. Their TG and DTG profiles are shown in Fig. 1. An inert material (e.g., soil or ceramics) dominates in the fines fraction, which is reflected by a small mass loss during the pyrolysis process (Fig. 1a). Consequently, due to its low degradability, Py-GC/MS analysis was not performed for this fraction. Fig. 2 shows the pyrovolpours composition for the analysed fractions, and Table 2 shows the main detected compounds in the pyrovolpours. The detected compounds were

Table 1
The parameters of the Py-GC/MS analysis.

Sample	T _{PYR} , °C	T _{CH} , °C	t _{PYR} , s	GC/MS programme	m/z range
2D plastic	501	200	6	holding at 40°C for 2 min, heating with 3 K/min to 280°C, and holding for 20 min	45-550
3D plastic	286	175	18		32-38 for the first 2 min and then 45-550
			6		
paper	498	175	6	holding at 40°C for 2 min, heating with 5 K/min to 280°C, and holding for 3 min	31-35 for the first 2 min and then 45-500
wood	512	175	6		45-550
rest	300	200	18	holding at 45 °C for 5 min, heating with 4 K/min to 280°C	31-35 for the first 5 min and then 45-500
	493		6		
textile	488	175	6	holding at 45 °C for 5 min, heating with 5 K/min to 280°C	31-35 for the first 5 min and then 45-500

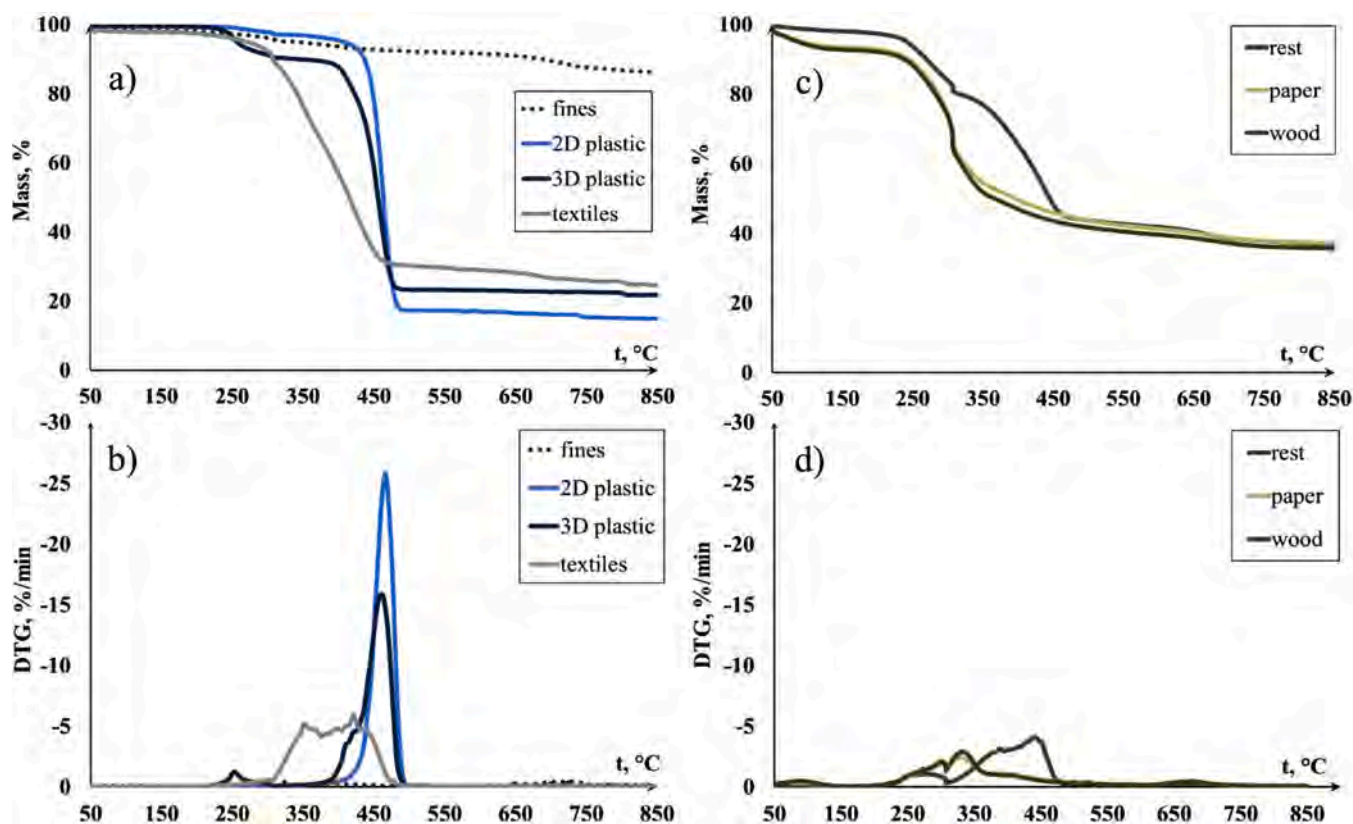


Fig. 1. TG (a, c) and DTG (b, d) profiles for analysed fractions of excavated wastes under a nitrogen atmosphere.

divided into twelve main groups. The definition of these groups, along with the list of all identified compounds, can be found in Tab. A2-9 in the Supplementary material. Additionally, Fig. 3 presents the summary of the TG and Py-GC/MS analyses in the form of material composition of the analysed fractions.

3.1.1. The 2D plastic fraction

One regular peak can be observed for the 2D plastic in the temperature range of 400 to 480 °C (Fig. 1c). The one-step decomposition pattern within a narrow temperature range coincides with the literature data on PE (both LDPE and HDPE), PP and PET decomposition (Breyer

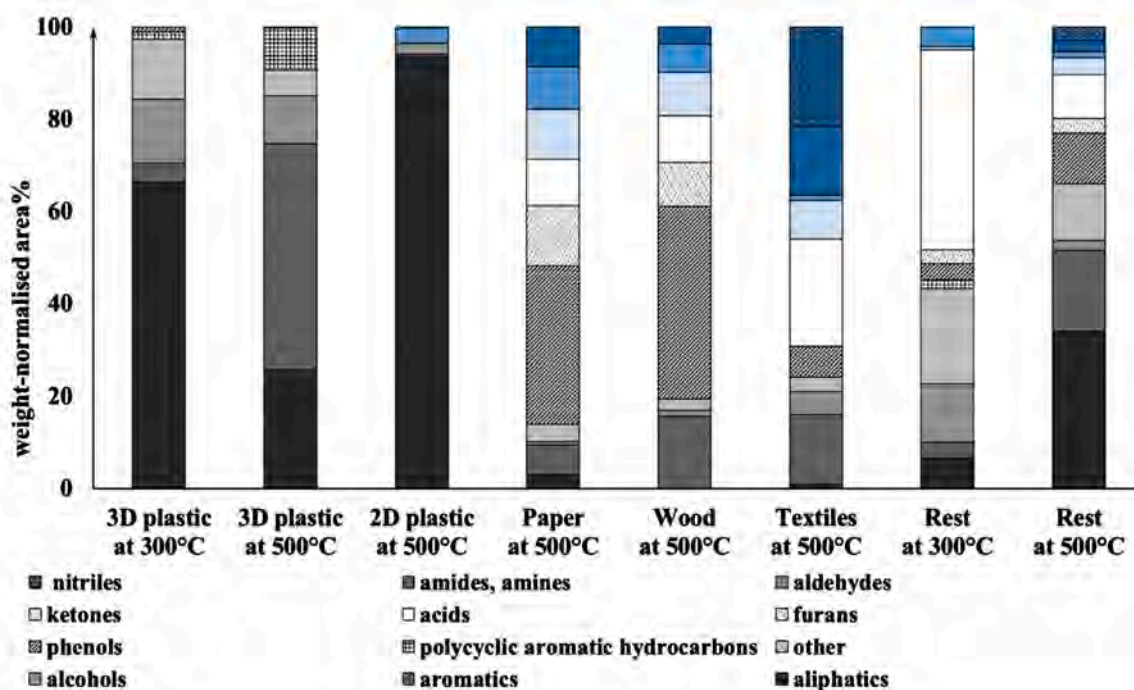


Fig. 2. The composition of pyrovolatiles for different excavated fractions.

Table 2
The main components detected in the pyrovapours.

Fraction	2D plastic	3D plastic at 300 °C	3D plastic at 500 °C	Paper
Content altogether, weight-normalised area%	Hex-1-ene	Hexacosane	Styrene	4-Vinylguaiacol
	1,2-Dimethylcyclopentane	Tetracosane	Benzene	Isoeugenol
	Dodec-1-ene	Hexadecan-1-ol	Heptadec-1-ene	D-Allose
	Dec-1-ene	Docosane	Heptacosan-1-ol	Vanillin
	Tetradec-1-ene	Squalene	Toluene	Guaiacol
	<u>35.9</u>	<u>63.8</u>	<u>49.2</u>	<u>35.6</u>
Fraction	Wood	Textiles	Rest at 300 °C	Rest at 500 °C
Content altogether, weight-normalised area%	Styrene	Azepan-2-one	Hexadecanoic acid	Cyclooctatetraene
	2,6-Dimethoxyphenol	2-Methylidene-pentamethylenemalonitrile	2-Ethylhexan-1-ol	2,4-Dimethylhept-1-ene
	2,6-Dimethoxy-4-prop-2-enylphenol	Hexadecanoic acid	2,4-Diisocyanato-1-methylbenzene	Levoglucosan
	4-Vinylguaiacol	Benzoic acid	1,3-Diisocyanato-2-methylbenzene	Hexadecanoic acid
	Isoeugenol	Cyclopentanone	Octadec-9-enoic acid	Benzoic acid
	<u>41.2</u>	<u>51.3</u>	<u>60.9</u>	<u>43.7</u>

et al., 2017; Diaz Silvarrey and Phan, 2016; Sørsum et al., 2001). Therefore, based on the TG results, it can be concluded that these three types of plastics dominate in the 2D plastic fraction. However, the performed Py-GC/MS analysis indicates the presence of only two of them – PE and PP, where PE significantly dominates. Following (Bockhorn et al., 1999; Williams and Williams, 1999) the main products of PE pyrolysis are linear alkanes and alkenes, whereas PP pyrolysis – usually-branched alkenes and, in the significantly smaller amount, usually-branched alkanes. The pyrovapours from the 2D plastic pyrolysis are characterised by a high aliphatics content in which linear alkenes and alkanes (approx. 59% and 25% of the total weight normalised area, respectively) dominate. Moreover, no typical PET pyrolysis products, such as Benzoic acid, Vinyl benzoate, Monovinyl terephthalate or Divinyl terephthalate (Brems et al., 2011; Sophonrat et al., 2017), were detected. Consequently, the presence of PET in the 2D plastic fraction was excluded.

A slight amount of oxygenated compounds (alcohols and aldehydes) was detected as well (up to 6% of the total weight normalised area%). This may be the consequence of the degradation of plastic, which leads to the formation of hydroxyl and carbonyl groups (Canopoli et al., 2020; Gijssman et al., 1999). Also, PP is more sensitive to oxidation (Gijssman et al., 1999; Moldovan et al., 2012); thereby, the detected oxygenates may originate mainly from its pyrolysis.

Summarising the above, PE and PP co-exist in the 2D plastic fraction, and PE is the predominant component (Fig. 3).

3.1.2. The 3D plastic fraction

On the contrary to the 2D plastic, the 3D plastic fraction is characterised by a two-step decomposition pattern (Fig. 1b). A small peak in the lower temperature range (225–300 °C) followed by a main asymmetric peak at 390–500 °C can be observed. The first degradation step can partially be related to PVC decomposition, which occurs at 200–380 °C (Park et al., 2012; Sørsum et al., 2001). Furthermore, the asymmetry of the second (main) peak indicates an overlapping of the decomposition of different plastic, namely PE, PP, PET, but also PS, which decomposes at 380–400 °C (Breyer et al., 2017; Sørsum et al., 2001). To sum up, the TG results show that the 3D plastic fraction is characterised by a more heterogeneous composition than the 2D plastic. Specifically, PVC, PE, PP, PET and PS may be found in this fraction.

Indeed, the Py-GC/MS results confirmed the presence of PVC in the 3D plastic fraction. According to (Yu et al., 2016) PVC decomposes stepwise with a dehydrochlorination at low temperatures (around 300 °C) followed by a cracking and decomposition of the remaining part at higher temperatures. The results show that the formation of HCl was detected (Fig. 3). Chlorobenzenes, the main chlorinated

hydrocarbons from PVS pyrolysis (Bhaskar et al., 2006; Yu et al., 2016), were detected at 300 °C as well. At 500 °C, moreover, a high amount of Benzene was detected (approx. 17% of the total weight-normalised area – Table 2), which is considered to be the main product of PVC pyrolysis at higher temperatures (Bhaskar et al., 2006; Yu et al., 2016).

An abundance of aliphatics was detected at 300 °C (Fig. 2), of which the majority consisted of linear C₁₈₋₂₈ alkanes (approx. 66% of the total weight-normalised area). This indicates that a partial PE decomposition occurred, which likely was accelerated by interactions with other plastics in the fraction (Singh et al., 2020; Williams and Williams, 1999). The linear alkanes are followed by alcohols (approx. 14% of the total weight-normalised area) and branched alkenes (approx. 9% of the total weight-normalised area). As mentioned before, branched alkenes and oxygenates are usually products of a PP decomposition since it is more prone to degrade than PE (Gijssman et al., 1999; Moldovan et al., 2012). Therefore, the detection of these compounds indicates that PP is present in larger amounts in the 3D plastic compared to the 2D plastic.

An intensive PS decomposition can also be seen at 500 °C, when the content of its main pyrolysis product, styrene, significantly increases (approx. 19% of the total weight-normalised area – Table 2). On the contrary, no common PET pyrolysis products were detected (Benzoic acid, Vinyl benzoate or Mono- and Divinyl terephthalate (Brems et al., 2011; Sophonrat et al., 2017)). Therefore, its presence in the analysed fraction was excluded, as in the case of the 2D plastic.

Given the above, it can be concluded that the PVC, PE, PP and PS are present in the 3D plastic fraction, whereas the presence of PET was excluded (Fig. 3).

3.1.3. The paper and wood fractions

The wood and paper decomposition follows nearly the same pattern (Fig. 1c-d) - two merged peaks can be observed in the range of 280–480 °C with the local maxima at 300 °C and 335 °C. This coincides with the available literature data, where the lignocellulosic biomass decomposes in the temperature range of 230–400 °C with two maxima at 291 °C and 330 °C (Ratnasari et al., 2019). Those two merged peaks can be attributed to the holocellulose decomposition (Sørsum et al., 2001). Moreover, a flat peak tailing above 350 °C can be observed as well, which may be related to the lignin decomposition (Sørsum et al., 2001).

The high content of phenols in the pyrovapours (Fig. 2), derived mainly from lignin (Jagodzińska et al., 2019a), indicates an extensive lignin degradation. This may be related to the high degradation degree of lignin (Mattonai et al., 2019), which depletes its thermal stability. Moreover, a low content of the primary holocellulose pyrolysis products

was detected (sugars, anhydrosugars, Levoglucosan and Levoglucosone, marked in Fig. 2 as *Other*). Those compound are considered to be abundant during the holocellulose degradation process as well (Fazio et al., 2020; Mattonai et al., 2017). This may indicate a significant degradation degree of holocellulose, which leads to the formation of lower-mass molecules.

In addition, a considerable amount of styrene was detected in the products of the wood pyrolysis (approx. 15% of the total weight-normalised area – Table 2), which suggests that PS is present in the fraction and that it also may contribute to the aforementioned peak tailing at higher temperatures. On the contrary, no styrene was detected among pyrovapours from the *paper* fraction. However, the *paper* pyrolysis results in the H₂S formation (Fig. 3).

Given the above, it may be concluded that the *wood* and *paper* fractions are characterised by a high degradation degree and that they may be contaminated by, for instance, PS (Fig. 3).

3.1.4. The textiles fraction

The *textiles* fraction decomposes in one step in the temperature range of 300 to 470 °C (Fig. 1a-b). The temperature range is in agreement with available literature data, for instance, for acrylic textile fabric waste (Nahil and Williams (2010)) or commingled waste textile fibre (Balci-Canbolat et al., 2017). On the contrary to the analysed fraction, these two studies indicate that the textile waste decomposition took place in two steps. Therefore, it can be concluded that the *textiles*' decomposition pattern in the form of one broad peak is a consequence of the overlapping of several different peaks and possible interactions of compounds within the fraction. As an example of merging the peaks in the case of textiles mixtures, (Miranda et al., 2007) show three-step decomposition pattern for used cotton fabrics, whereas (Yousef et al., 2019) show the two-stage decomposition of waste jeans being a mixture of cotton and polyester.

The combined decomposition pattern suggests that this fraction has a heterogenic composition. Specifically, the Py-GC/MS analysis indicates the presence of several materials in the fraction. The main detected compound is Caprolactam (approx. 15% of the total weight-normalised area – Table 2), which is the key product of Nylon 6 pyrolysis (Lehrle et al., 2000). Moreover, the high content of nitriles (Fig. 2), especially mononitriles, indicates the presence of other polyamides such as Nylon 12 (Ohtani et al., 1982; Wu et al., 2013). No sulphur-containing compounds were detected among the pyrovapours except for H₂S (Fig. 3).

A slight content of Levoglucosan, which is the primary product of cellulose pyrolysis, was detected in the fraction as well. This suggests that cellulose-fibres, like, e.g. linen, viscose or cotton, are present in the sample despite the long time the materials have been buried in the ground. The relatively high content of oxygenated compounds (ketones and acids) confirms their presence as well (Zhu et al., 2004). Additionally, the relatively high contents of fatty acids (approx. 15% of the total weight-normalised area – Table 2.) may also indicate the presence of wool (Asperger et al., 1999; Sabatini et al., 2018).

Summarising the above, the *textiles* fraction is composed of both synthetic (polyamides like Nylon 6 and 12) and natural fibres (cellulose-fibres like linen, viscose, cotton or wool) (Fig. 3).

3.1.5. The rest fraction

Visually, the so-called *rest* fraction consists of rubber, foam, and other unidentified compounds. It decomposes in two steps at 225–310 °C and 310–480 °C (Fig. 1c-d). A slight mass loss occurs around 615–700 °C (Fig. 1c-d) and can be attributed to the decomposition of impurities of the sample. This can, for instance, be CaCO₃, which decompose at higher temperatures (Garrido and Font, 2015).

The aforementioned two decomposition steps can partially be related to the rubber content. (Chen and Qian, 2003; Kan et al., 2017; Wang et al., 2014) studied waste black rubber pyrolysis and indicated three

main stages of its thermal decomposition. The first stage (200–350 °C) was connected to the pyrolysis of oils, plasticisers and other additives, followed by the decomposition of natural (NR) and styrene-butadiene rubber (SBR) at 350–450 °C. Finally, the third stage was the butadiene rubber (BR) decomposition at 400–500 °C.

No styrene and styrene derivatives were detected in the Py-GC/MS experiments. Therefore, the presence of SBR in the sample was excluded. However, the Py-GC/MS results indicated the presence of thiophenes and thiazoles, which are considered to be typical pyrolysis products of sulphur cross-linked rubbers (Kaminsky and Mennerich, 2001). The derivative of the commonly used vulcanising agent, benzothiazole, was also detected among the pyrovapours at 300 °C (Choi et al., 2014). This suggests that natural rubber is present in the fraction since it is characterised by lower thermal stability than BR, which also has been depleted because of ageing. At 500 °C, on the contrary, Benzenitrile was detected. This can be used to identify a nitrile-butadiene rubber (NBR) presence in the sample (Fuh and Wang (1998)). A relatively high thermal stability characterises NBR, despite the ageing (Liu et al., 2016), thereby is likely to decompose at higher temperatures than natural rubber.

The abundance of Cyclooctatetraene at 500 °C (Table 2) may be related either to plastic fraction content (Park et al., 2012) or rubber pyrolysis, since cycloaliphatics are often found among rubber pyrolysis products as a result of Diels-Alder reactions (Kaminsky and Mennerich, 2001; Kan et al., 2017).

The *rest*'s decomposition steps are also related to the decomposition of foam-like materials – the first step can be seen at lower temperatures, whereas the second step is overlapping with the rubber decomposition. (Font et al., 2001) investigated pyrolysis of pure polyurethane foam and determined the temperature range of 250–350 °C as its primary decomposition step. On the other hand, (Jiao et al., 2013) studied rigid polyurethane (PU) foam (building insulation) pyrolysis, which decomposed at 220–400 °C with a tailing pronounced shoulder until 600 °C, whereas (Garrido and Font, 2015) studied the pyrolysis of the waste mattresses. They found that the waste mattresses decomposed at 225–325 °C and 350–450 °C. Those temperature ranges may suggest that the *rest* fractions consist not only of pure PU but also of other types of foam-materials.

Indeed, the presence of polyurethane foam (PU) in the *rest* fraction was detected by Py-GC/MS. As mentioned before, PU decomposes in two steps. The first step occurs at lower temperatures (200–325 °C) and results in the formation of isocyanate derivatives (Garrido and Font, 2015; La Nasa et al., 2018). The abundance of two isocyanates, namely 2,4-Diisocyanato-1-methylbenzene and its rearranged molecule 1,3-Diisocyanato-2-methylbenzene, was detected at 300 °C (Table 2). Moreover, the formation of hydrazine (Fig. 3), used in chemical foaming agents, additionally confirms that PU is present in the sample. Furthermore, PU decomposition results in the formation of aliphatic alcohols with branched chains as well as benzene alkyls, mainly at higher temperatures. Indeed 2-Ethylhexan-1-ol was detected at temperatures of 300 °C and 500 °C (Tab. 2), whereas Toluene, xXylene and Ethylbenzene were detected at 500 °C. This confirms the presence of PU in the *rest* fraction.

The high acids content at 300 °C and phenols content at 500 °C (Fig. 2), combined with detection of anhydrosugars, Levoglucosone and Levoglucosan, suggest the presence of lignocellulosic materials in the fraction (Jagodzińska et al., 2019b).

To sum up, the *rest* fraction consists predominantly of polyurethane foam, different types of rubber (e.g., natural and nitrile-butadiene rubber), and lignocellulosic materials (Fig. 3).

3.2. Calorific value, proximate and elemental analysis

Seven excavated waste fractions (2D plastic, 3D plastic, paper, rest, textile, wood, fines (<20 mm)) were subjected to the proximate and elemental analysis along with the determination of their gross calorific

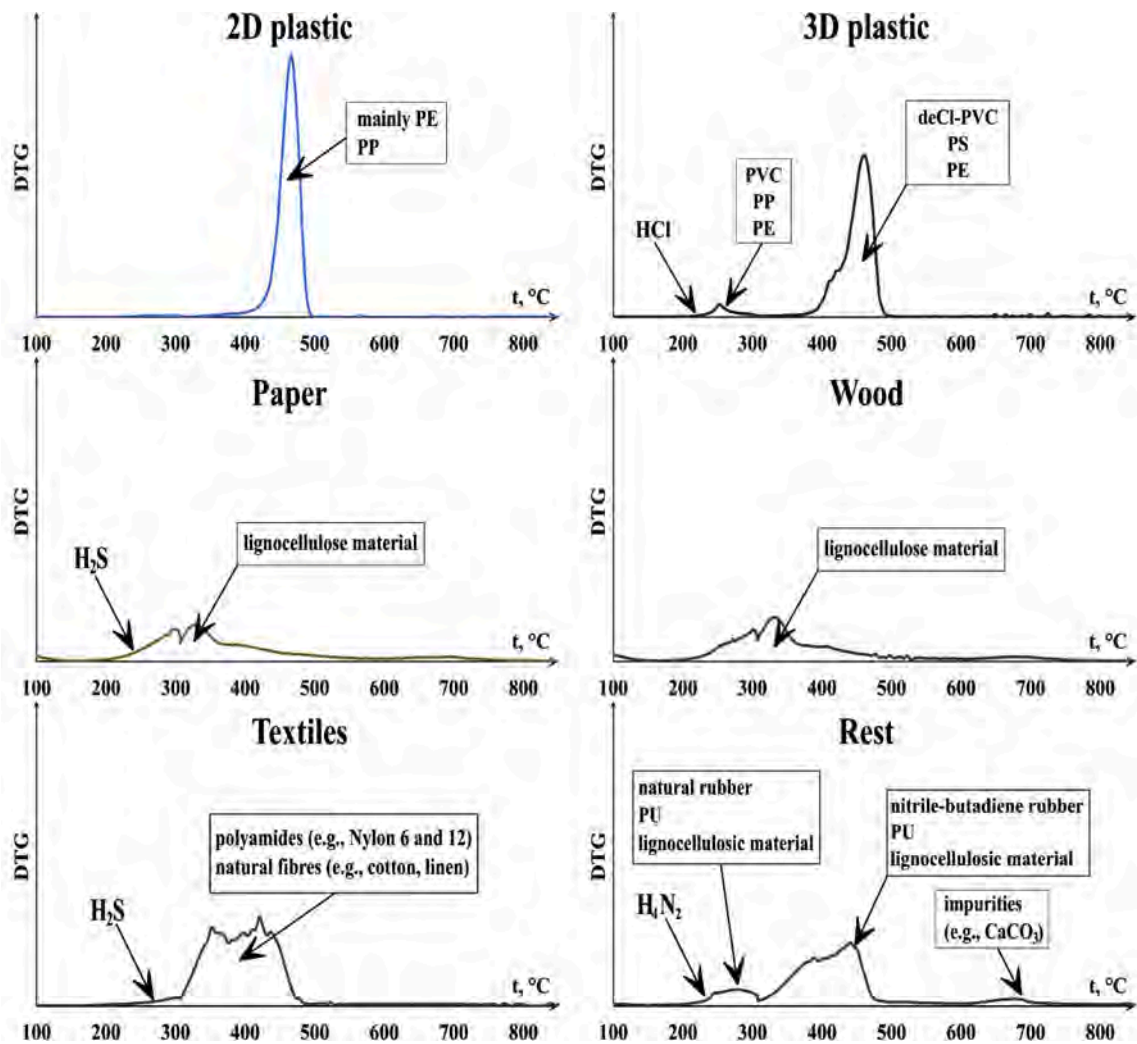


Fig. 3. The material composition of the analysed fractions.

values (Fig. 4–5). The exact values are shown in Tab. A10–11 in the Supplementary material. In general, the results show high contamination of the analysed fractions with heavy metals (a significant content of Hg is especially noticeable) and other impurities (i.e., soil-like material or small Cu particles), which has its reflection in their high ash content. Moreover, the chlorine and sulphur contents in the fractions are higher than that of fresh waste (Sieradzka et al., 2020), but similar to the results for other excavated waste (Kaartinen et al., 2013; Quaghebeur et al., 2013; Zhou et al., 2014).

A high calorific value characterises the *2D plastic* and *3D plastic* fractions (Fig. 4b), yet still, it is lower than that of raw plastics (Panda et al., 2010). The decrease in calorific value is related to the elevated ash content in the *2D plastic* fraction, due to the impurities attached to the surface of the particles and the high chlorine content in the *3D plastic* fraction (Fig. 4a). Notwithstanding that, the analysed fractions have higher calorific values than most of other excavated plastics reported elsewhere (Quaghebeur et al., 2013; Wolfsberger et al., 2015) except for (Zhou et al., 2014) who noted almost no decrease of the calorific value of plastics excavated from the Yingchun landfill in China in comparison to fresh plastic waste. The analysed plastic fractions are also characterised by lower Ba, Cd, Cr, Cu (*2D plastic*), Ni, Pb, and Zn contents, and a significantly higher Hg content, comparing to the studies of (Prechthai et al., 2008; Quaghebeur et al., 2013; Wolfsberger et al., 2015) (Fig. 5b–d). The high content of Hg may be related to the small particles of batteries,

thermometers or bulbs adhered to the soft surface of plastics subjected to the mechanical stress from upper layers. The *3D plastic* fraction is also characterised by considerable contents of Sb and Cu (Fig. 4b and d), likely related to the presence of flame retardants and copper wire remaining in the pieces of cable insulation manually classified to the plastic fraction. Moreover, the high chlorine content in this fraction confirms the findings of the TG and Py-GC/MS analyses indicating a considerable amount of PVC among the *3D plastic* (Fig. 3). On the contrary, the *2D plastic* fraction is characterised by high contents of Al, Ca, Fe and Si (Fig. 5a), which is a direct consequence of its contamination with soil-like impurities, which is also reflected by the aforementioned high ash content in this fraction.

The relatively high calorific values of the *paper* and *wood* fractions (Fig. 4a) coincide with the findings of (Wolfsberger et al., 2015). However, the *paper* contains smaller amounts of Ba, Cr, Cu, Ni, Pb and Zn, and the *wood* contains lower amounts of Cr and Ni than reported by (Quaghebeur et al., 2013; Wolfsberger et al., 2015) (Fig. 4b–d). Despite the apparent lower contamination of those fractions, they contain an extensive amount of Hg (Fig. 4d), which drags them into a potentially hazardous waste group. Especially the *wood* fraction has the highest Hg content among all of the analysed fractions (17.2 ± 5.2 mg/kg).

The significant ash content characterises the *textiles* fraction resulting in its relatively low calorific value (Fig. 4a–b). Its high

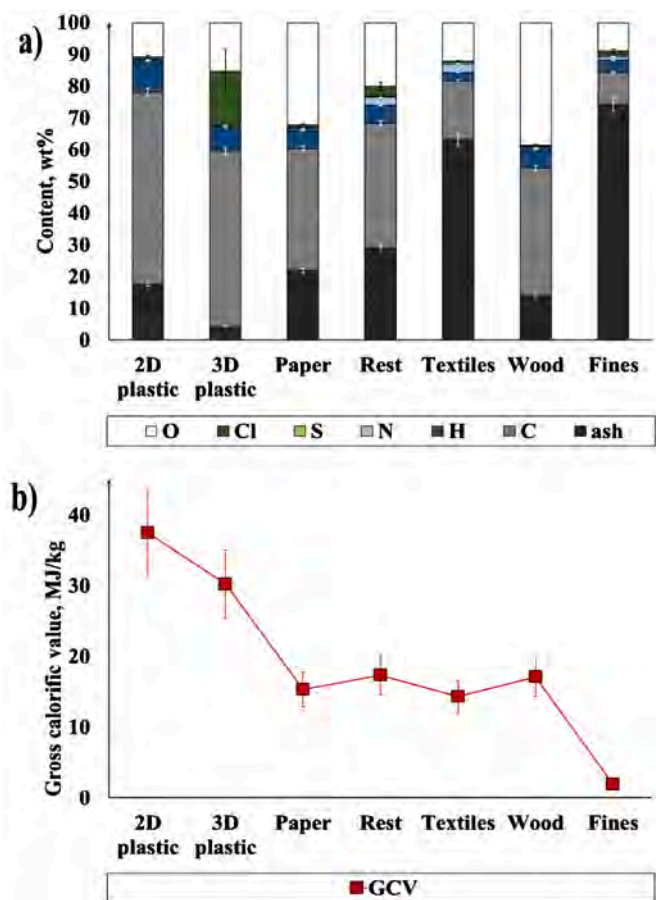


Fig. 4. The results of proximate and elemental analysis of the analysed fractions (a) as well as their gross calorific value in a dry state (b).

contents of Al, Ca, Fe, and Si reflect the presence of soil-like material in the textiles fraction (Fig. 5a). Moreover, the content of Cr, Hg and Pb exceeds that reported by (Wolfsberger et al., 2015), whereas the V and Sb contents exceed that of refuse-derived fuel considered as being rich in those elements (Jagodzińska et al., 2019c). This indicates a high contamination level of this fraction. Similarly, the rest fraction is not only characterised by high contents of Cr, Hg, Pb and Sb but also by high contents of Zn and Cl, which indicates its high contamination as well. Furthermore, the high content of nitrogen characterises both of those fractions (Fig. 4a), which coincides with the TG and Py-GC/MS results on great content of polyamides (the textiles) and PU (the rest) in those fractions (Fig. 3).

As mentioned before, the fines fraction contains mostly soil-like material, thereby having a high ash content and, consequently, low calorific value (Fig. 4a-b). This fraction also contains an excessive amount of Cd, Hg and Pb (Fig. 5c-d) in comparison to values reported in (Parrodi et al., 2020, 2018; Wolfsberger et al., 2015). The elevated Cd and Pb contents may be related to glass particles present in the fraction, since Cd and Pb were used as colourants and decorative agents for glass (Parrodi et al., 2020). The high Hg content may be related to the aforementioned small particles of bulbs, thermometers and batteries present in the fraction.

Summarising the above, all of the analysed fractions contain undesirable compounds both with respect to material or energy recoveries. Therefore, the following section discusses the possible ways of their utilisation, taking into account the aggregate data obtained hitherto.

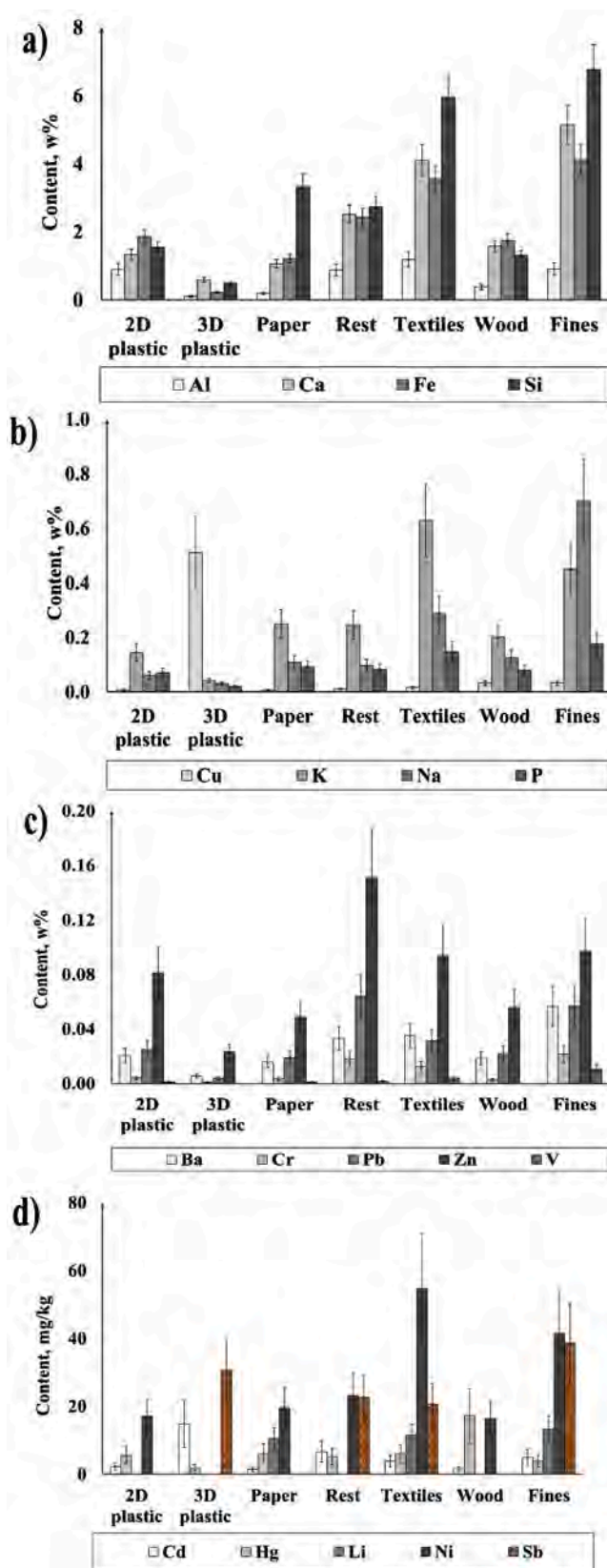


Fig. 5. The results of ICP analysis of the analysed fractions.

3.3. Discussion on the potential utilisation of the excavated waste fractions

Based on the outcomes of the above characterisation of individual fractions, their possible further applications have been preliminarily assessed.

There are three main ways of waste recycling, namely primary, secondary and tertiary recycling. Primary recycling assumes the production of a new product from waste without or with a slight quality loss, whereas secondary recycling assumes the production of lower-quality goods from waste (i.e., piping or packaging materials produced from waste plastics). However, primary and secondary recycling is rather inaccessible for the majority of analysed fractions due to their highly heterogeneous compositions (*3D plastic, textile, rest* in Fig. 3) and contamination with inert materials (*paper, rest, textiles, wood* in Fig. 4a). Moreover, all of those fractions contain a considerable amount of hazardous heavy metals, especially Hg and Pb (Fig. 5c-d). Only, the *2D plastic* fraction is characterised by a relatively homogenous composition; however, its quality is not sufficient for the primary recycling due to its degradation manifested by the presence of oxygenated compounds among its pyrolysis products (Fig. 2). Furthermore, the *2D plastic* fraction is characterised by high ash and heavy metals content (Fig. 4-5), exceeding the limit for, for instance, material which can be used in packaging, according to European Parliament and Council Directive 94/62/EC. The washing step, however, may reduce heavy metals content significantly (Parrodi et al., 2018); therefore, secondary recycling seems applicable for this fraction, yet demands more extensive analysis.

Given the above obstacles related to primary and secondary recycling of excavated waste fractions, tertiary recycling seems to be the most appropriate route of energy and material recovery from those waste. Indeed, the analysed fractions are characterised by a relatively high calorific value, which indicates the feasibility of their waste-to-energy application. However, none of them met the requirements set for solid-recovered fuel in the EN 15359:2012 standard owing to their high Hg content (Fig. 5d), and, in the case of the *3D plastics* and the *rest* fractions, also their high Cl content (Fig. 4a). In countries which environmental legislation includes limits for the content of other heavy metals, such as Austria (Parrodi et al., 2020), all of the analysed fractions exceed the limits set for Cd and Pb content. Therefore, they would need to be subjected to a washing process prior to its incineration to remove contaminants, which makes the feasibility of this process uncertain.

Pyrolysis can constitute a valorisation route alternative to incineration. The obtained aliphatic compounds from the *2D plastic* pyrolysis (Fig. 2) are not of commercial interest, but they have a high potential for selective pyrolysis (Lopez et al., 2017) or catalytic upgrading to fuel or high-quality syngas (Barbarias et al., 2016; Erkiaga et al., 2015). Therefore, pyrolysis of this fraction seems to be a feasible way of its valorisation. On the contrary, the *3D plastic* pyrolysis is connected with increased corrosiveness of the process products, due to the extensive formation of HCl (Fig. 3) and the presence of chlorine-containing compounds among condensable volatiles. Therefore, either cleaning of the produced pyrogas or stepwise pyrolysis would be needed (Sophonrat et al., 2019). The stepwise pyrolysis enables the separation of the majority of undesirable components, which are produced at a lower temperature (300 °C), before catalytically upgrading the pyrolysis products formed at a higher temperature (500 °C). However, both the pyrogas cleaning or the stepwise pyrolysis, demands higher operational and investments costs. These factors reduce the feasibility of the proposed solution.

The *paper* and *textiles* pyrolysis results in the formation of H₂S (Fig. 3) and, in the case of the *textiles*, also chlorine-containing condensable volatiles. This downgrades the quality of the process products and increases their corrosiveness. Similarly, the pyrolysis of the *rest* fraction is connected to the formation of toxic hydrazine (Fig. 3) and sulphur-containing condensable compounds, whereas the *wood* pyrolysis is

related to releasing high amounts of gaseous Hg. Therefore, cleaning of the produced pyrogas would be necessary before its further utilisation.

The *finer* contain more nutrients (K, Na and P) than the other analysed fractions; however, still, their content is not sufficient for using it as compost (Prechthai et al., 2008). Moreover, its contamination with Cd, Pb and Hg may cause its toxicity when used as compost or in other environmental utilisations (Fig. 5c-d). On the other hand, the *finer* may constitute a source of rare metals, including Ba, Cr, Co, Li, Ni, Mn, Sb, Ti and V (Gutiérrez-Gutiérrez et al., 2015; Kamura et al., 2019). However, the relatively low content of the listed metals in the *finer* excludes feasibility of urban mining in this case. The *finer* could also be utilised as a construction material according to the Flemish VLAREA guidance for the use of waste as construction materials (Quaghebeur et al., 2013). However, to fully assess their potential, the leachability tests would be necessary to investigate the mobility of heavy metals.

To sum up, finding a suitable valorisation way for all of the analysed fractions is challenging. For most of the analysed fractions, material recovery is impossible due to their heterogeneous composition and high content of different types of impurities (among others soil-like material and heavy metals). Nonetheless, they are characterised by a high calorific value, which advocates for their energy use. Selective or catalytic pyrolysis seems to be a feasible way of the *2D plastic* fraction valorisation due to its relatively homogenous composition. On the contrary, pyrolysis of other analysed fractions is connected with numerous technical complications related to the presence of corrosive and toxic compounds among produced pyrovapours which hinders the process feasibility. Therefore, two directions could be taken in future research. First of them is the production of valuable chemicals, fuel or syngas from the *2D plastic* fraction. Second of them is the maximisation of the rate of all fractions utilisation by their collective pyrolysis, which would also result in the reduction of sorting costs by avoiding an extra separation step.

4. Conclusions

First of all, seven fractions of the excavated material (two plastic fractions, wood, paper, textiles and the remaining unclassified fraction referred to as the *rest* fraction) were characterised in terms of their material and elemental composition. Afterwards, their possible utilisation was discussed. Overall, the main findings of the study can be summarised as follows:

- 1 A highly heterogeneous composition characterises most of the analysed fractions - the *3D plastic* fraction contains different types of plastics (PVC, PE, PP, PS), the *textiles* fraction consist of both synthetic and natural textiles, whereas the *rest* fraction predominantly contains polyurethane foam and different types of rubber. The exception of this is the *2D plastic* fraction consisting mainly of PE; therefore, the secondary recycling of this fraction seems applicable.
- 2 The *finer* fraction contains considerable amounts of heavy metals which hinders its using as compost or in other environmental utilisations. However, it might be used as a construction material; therefore, investigation of the heavy metals leachability from the *finer* fraction would be necessary.
- 3 The analysed fractions are characterised by high calorific values, but contain high amounts of heavy metals (especially Hg) and Cl, which may demand pre-treatment (i.e., washing) prior to their incineration and may potentially result in the unprofitability of their incineration.
- 4 Pyrolysis seems to be a feasible way of utilising the fractions although for most of them it is connected with some technical complications (i.e., the presence of toxic and corrosive compounds among formed pyrovapours may require cleaning prior to their use).

Given the above, further research following three paths shall be considered: I – a feasibility study of secondary recycling of the *2D plastic* fraction and using the *finer* as construction material, II – further research on selective or catalytic pyrolysis of the *2D plastic* fraction individually,

and III – further research on the pyrolysis of all analysed fractions collectively.

Declaration of Competing Interest

None.

Acknowledgement



The NEW-MINE project has received funding from

the European Union's Horizon 2020 research and innovation programme under the Marie Skłodowska-Curie grant agreement No 721185. The project website is <http://new-mine.eu/>.

Supplementary materials

Supplementary material associated with this article can be found, in the online version, at [doi:10.1016/j.resconrec.2021.105446](https://doi.org/10.1016/j.resconrec.2021.105446).

References

- Agon, N., Hrabovský, M., Chumak, O., Hlína, M., Kopecký, V., Mašláni, A., Bosmans, A., Helsen, L., Skoblja, S., Van Oost, G., Vierendeels, J., 2016. Plasma gasification of refuse derived fuel in a single-stage system using different gasifying agents. *Waste Manag.* 47, 246–255. <https://doi.org/10.1016/j.wasman.2015.07.014>.
- Arshad, K., Mujahid, M., 2011. Biodegradation of Textile Materials. University of Borås.
- Asperger, A., Engewald, W., Fabian, G., 1999. Analytical characterization of natural waxes employing pyrolysis-gas chromatography–mass spectrometry. *J. Anal. Appl. Pyrolysis* 50, 103–115.
- Balcik-Canbolat, C., Ozbey, B., Dizge, N., Keskinler, B., 2017. Pyrolysis of commingled waste textile fibers in a batch reactor: analysis of the pyrolysis gases and solid product. *Int. J. Green Energy* 14, 289–294. <https://doi.org/10.1080/15435075.2016.1255634>.
- Barbarias, I., Lopez, G., Artetxe, M., Arregi, A., Santamaria, L., Bilbao, J., Olazar, M., 2016. Pyrolysis and in-line catalytic steam reforming of polystyrene through a two-step reaction system. *J. Anal. Appl. Pyrolysis* 122, 502–510. <https://doi.org/10.1016/j.jaap.2016.10.006>.
- Bhaskar, T., Negoro, R., Muto, A., Sakata, Y., 2006. Prevention of chlorinated hydrocarbons formation during pyrolysis of PVC or PVDC mixed plastics. *Green Chem* 8, 697–700. <https://doi.org/10.1039/b603037h>.
- Bockhorn, H., Hornung, A., Hornung, U., Schwallier, D., 1999. Kinetic study on the thermal degradation of polypropylene and polyethylene. *J. Anal. Appl. Pyrolysis* 48, 93–109. [https://doi.org/10.1016/S0165-2370\(98\)00131-4](https://doi.org/10.1016/S0165-2370(98)00131-4).
- Bosmans, A., De Dobbelaere, C., Helsen, L., 2014. Pyrolysis characteristics of excavated waste material processed into refuse derived fuel. *Fuel* 122, 198–205. <https://doi.org/10.1016/j.fuel.2014.01.019>.
- Brand, J.H., Spencer, K.L., 2018. Risk screening assessment for ranking historic coastal landfills by pollution risk. *Anthr. Coasts* 1, 44–61. <https://doi.org/10.1139/anc-2018-0001>.
- Brems, A., Baeyens, J., Vandecasteele, C., Dewil, R., 2011. Polymeric cracking of waste polyethylene terephthalate to chemicals and energy. *J. Air Waste Manag. Assoc.* 61, 721–731. <https://doi.org/10.3155/1047-3289.61.7.721>.
- Breyer, S., Mekhitarian, L., Rimez, B., Haut, B., 2017. Production of an alternative fuel by the co-pyrolysis of landfill recovered plastic wastes and used lubrication oils. *Waste Manag* 60, 363–374. <https://doi.org/10.1016/j.wasman.2016.12.011>.
- Canopoli, L., Coulon, F., Wagland, S.T., 2020. Degradation of excavated polyethylene and polypropylene waste from landfill. *Sci. Total Environ.* 698, 134125. <https://doi.org/10.1016/j.scitotenv.2019.134125>.
- Canopoli, L., Fidalgo, B., Coulon, F., Wagland, S.T., 2018. Physico-chemical properties of excavated plastic from landfill mining and current recycling routes. *Waste Manag* 76, 55–67. <https://doi.org/10.1016/j.wasman.2018.03.043>.
- Chen, F., Qian, J., 2003. Studies of the thermal degradation of waste rubber. *Waste Manag* 23, 463–467. [https://doi.org/10.1016/S0956-053X\(03\)00090-4](https://doi.org/10.1016/S0956-053X(03)00090-4).
- Choi, G., Jung, S., Oh, S., Kim, J., 2014. Total utilization of waste tire rubber through pyrolysis to obtain oils and CO₂ activation of pyrolysis char. *Fuel Process. Technol.* 123, 57–64. <https://doi.org/10.1016/j.fuproc.2014.02.007>.
- Ciuta, S., Tsiamis, D., Castaldi, M.J., 2017a. Field scale developments, in: Gasification of waste materials: technologies for generating energy, gas, and chemicals from municipal solid waste., *Biomass Nonrecycled Plast. Sludges Wet Solid Wastes* 65–91. <https://doi.org/10.1016/B978-0-12-812716-2.00004-2>.
- Ciuta, S., Tsiamis, D., Castaldi, M.J., 2017b. Economic summary, in: Gasification of Waste Materials: Technologies for Generating Energy, Gas, and Chemicals from Municipal Solid Waste., *Biomass Nonrecycled Plast. Sludges Wet Solid Wastes* 143–150. <https://doi.org/10.1016/B978-0-12-812716-2.00007-8>.
- Diaz Silvarrey, L.S., Phan, A.N., 2016. Kinetic study of municipal plastic waste. *Int. J. Hydrogen Energy* 41, 16352–16364. <https://doi.org/10.1016/j.ijhydene.2016.05.202>.
- Erkiaga, A., Lopez, G., Barbarias, I., Artetxe, M., Amutio, M., Bilbao, J., Olazar, M., 2015. HDPE pyrolysis-steam reforming in a tandem spouted bed-fixed bed reactor for H₂ production. *J. Anal. Appl. Pyrolysis* 116, 34–41. <https://doi.org/10.1016/j.jaap.2015.10.010>.
- Esguerra, J.L., Krook, J., Svensson, N., Van Passel, S., 2019. Assessing the economic potential of landfill mining: review and recommendations. *Detritus* 08, 125–140. <https://doi.org/10.31025/2611-4135/2019.13883>.
- European Commission, 2020. A new Circular Economy Action Plan for a cleaner and more competitive Europe. <https://doi.org/10.1017/CBO9781107415324.004>.
- Fazio, E., Corsaro, C., Mallamace, D., 2020. Paper aging and degradation monitoring by the non-destructive two-dimensional micro-Raman mapping. *Spectrochim. Acta Part A Mol. Biomol. Spectrosc.* 228, 117660. <https://doi.org/10.1016/j.saa.2019.117660>.
- Font, R., Fullana, A., Caballero, J.A., Candela, J., García, A., 2001. Pyrolysis study of polyurethane. *J. Anal. Appl. Pyrolysis* 58–59, 63–77. [https://doi.org/10.1016/S0165-2370\(00\)00138-8](https://doi.org/10.1016/S0165-2370(00)00138-8).
- Fuh, M.-R.S., Wang, G.-Y., 1998. Quantitative analysis of nitrile rubber chloroprene material by pyrolysis/gas chromatography/mass spectrometry. *Anal. Chim. Acta* 371, 89–96. [https://doi.org/10.1016/S0003-2670\(98\)00314-6](https://doi.org/10.1016/S0003-2670(98)00314-6).
- García Lopez, C., Ni, A., Parrodi, J.C.H., Küppers, B., Raulf, K., Pretz, T., 2019. Characterization of landfill mining material after ballistic separation to evaluate material and energy recovery potential. *Detritus* 08, 5–23. <https://doi.org/10.31025/2611-4135/2019.13780>.
- Garrido, M.A., Font, R., 2015. Pyrolysis and combustion study of flexible polyurethane foam. *J. Anal. Appl. Pyrolysis* 113, 202–215. <https://doi.org/10.1016/j.jaap.2014.12.017>.
- Ghosh, S., Sadhan Kumar, Levitzke, Vaughan, P.S.M., Nikzad, H., Tshomo, U., Dorji, C., Dahal, Y., Cocker, J., Graham, K., Zeng, X., Li, J., Nelles, M., Nassour, A., Morscheck, G., Chansomphou, V., Daskal, S., Ayalon, O., Di Maria, F., Koech, M. K., Munene, K.J., Agamuthu, P., Mehran, S.B., Kowlessar, P., Aremu, S.A., David O. Olukanni, Mokuolu, Olubunmi A., Lasode, Olumuyiwa A., Ahove, M.A., Ojowuro, O. M., Karstensen, K.H., Engelsens, Christian John Saha, P.K., Rhee, S.-W., Pavlović, M., Vulić, M., Pavlović, A., Tangwanichapong, S., Logan, Visvanathan, Mohanakrishnan, C., Farmer, A., Guran, S., Mersky, R.L., Ghosh, Sannidhya, K., Hai, H.T., Quang, N.D., Thang, N.T., Nam, N.H., 2020. Circular Economy: Global Perspective, Circular Economy: Global Perspective. Springer Nature Singapore Pte Ltd. 2020. <https://doi.org/10.1007/978-981-15-1052-6>.
- Gijsman, P., Meijers, G., Vitarelli, G., 1999. Comparison of the UV-degradation chemistry of polypropylene, polyethylene, polyamide 6 and polybutylene terephthalate. *Polym. Degrad. Stab.* 65, 433–441. [https://doi.org/10.1016/S0141-3910\(99\)00033-6](https://doi.org/10.1016/S0141-3910(99)00033-6).
- González Martínez, M., Ojra-aho, T., da Silva Perez, D., Tamminen, T., Dupont, C., 2019. Influence of step duration in fractionated Py-GC/MS of lignocellulosic biomass. *J. Anal. Appl. Pyrolysis* 137, 195–202. <https://doi.org/10.1016/j.jaap.2018.11.026>.
- Greisch, B., *détudes*, 2002. Centre d'Enfouissement Technique de Mont-Saint-Guibert: Etude des conséquences de l'octroi du permis d'urbanisme du 29.10.01 sur les conditions d'exploitation du permis du 16.12.98.
- Gutiérrez-Gutiérrez, S.C., Coulon, F., Jiang, Y., Wagland, S., 2015. Rare earth elements and critical metal content of extracted landfill material and potential recovery opportunities. *Waste Manag* 42, 128–136. <https://doi.org/10.1016/j.wasman.2015.04.024>.
- He, P., Chen, L., Shao, L., Zhang, H., Lü, F., 2019. Municipal solid waste (MSW) landfill: A source of microplastics? – Evidence of microplastics in landfill leachate. *Water Res* 159, 38–45. <https://doi.org/10.1016/j.watres.2019.04.060>.
- Hernández Parrodi, J.C., García-López, C., Küppers, B., Vollprecht, D., Pretz, T., Pomberger, R., 2019a. Case study on enhanced landfill mining at Mont-Saint-Guibert landfill in Belgium: characterization and potential of fine fractions. *Detritus*.
- Hernández Parrodi, J.C., Lucas, H., Gigantino, M., Sauve, G., Esguerra, J.L., Einhäupl, P., Vollprecht, D., Pomberger, R., Friedrich, B., Van Acker, K., Krook, J., Svensson, N., Van Passel, S., 2019b. Integration of resource recovery into current waste management through (enhanced) landfill mining 08, 141–156. <https://doi.org/10.31025/2611-4135/2019.13884>.
- Hogland, W., Marques, M., Nimmermark, S., 2004. Landfill mining and waste characterization: a strategy for remediation of contaminated areas. *J. Mater. Cycles Waste Manag.* 6, 119–124. <https://doi.org/10.1007/s10163-003-0110-x>.
- Jagodzińska, K., Czerep, M., Kudlek, E., Wnukowski, M., Yang, W., 2019a. Torrefaction of wheat-barley straw: Composition and toxicity of torrefaction condensates. *Biomass Bioenergy* 129, 105335. <https://doi.org/10.1016/j.biombioe.2019.105335>.
- Jagodzińska, K., Czerep, M., Kudlek, E., Wnukowski, M., Yang, W., 2019b. Torrefaction of wheat-barley straw: composition and toxicity of torrefaction condensates. *Biomass Bioenergy* 129, 105335. <https://doi.org/10.1016/j.biombioe.2019.105335>.
- Jagodzińska, K., Mroczek, K., Nowińska, K., Golombek, K., Kalisz, S., 2019c. The impact of additives on the retention of heavy metals in the bottom ash during RDF incineration. *Energy* 183, 854–868. <https://doi.org/10.1016/j.energy.2019.06.162>.
- Jiao, L., Xiao, H., Wang, Q., Sun, J., 2013. Thermal degradation characteristics of rigid polyurethane foam and the volatile products analysis with TG-FTIR-MS. *Polym. Degrad. Stab.* 98, 2687–2696. <https://doi.org/10.1016/j.polydegradstab.2013.09.032>.
- Johansson, N., Krook, J., Eklund, M., 2012. Transforming dumps into gold mines. Experiences from Swedish case studies. *Environ. Innov. Soc. Transitions* 5, 33–48. <https://doi.org/10.1016/j.eist.2012.10.004>.
- Jones, P.T., Geysen, D., Tielemans, Y., Van Passel, S., Pontikes, Y., Blanpain, B., Quaghebeur, M., Hoekstra, N., 2013. Enhanced Landfill Mining in view of multiple

- resource recovery: A critical review. *J. Clean. Prod.* 55, 45–55. <https://doi.org/10.1016/j.jclepro.2012.05.021>.
- Kaartinen, T., Sormunen, K., Rintala, J., 2013. Case study on sampling, processing and characterization of landfilled municipal solid waste in the view of landfill mining. *J. Clean. Prod.* 55, 56–66. <https://doi.org/10.1016/j.jclepro.2013.02.036>.
- Kaminsky, W., Mennerich, C., 2001. Pyrolysis of synthetic tire rubber in a fluidised-bed reactor to yield 1,3-butadiene, styrene and carbon black. *J. Anal. Appl. Pyrolysis* 58–59, 803–811. [https://doi.org/10.1016/S0165-2370\(00\)00129-7](https://doi.org/10.1016/S0165-2370(00)00129-7).
- Kamura, K., Omori, M., Kurokawa, M., Tanaka, H., 2019. Estimation of the potential of landfill mining and exploration of metal-enriched zones. *Waste Manag* 93, 122–129. <https://doi.org/10.1016/j.wasman.2019.04.050>.
- Kan, T., Strezov, V., Evans, T., 2017. Fuel production from pyrolysis of natural and synthetic rubbers. *Fuel* 191, 403–410. <https://doi.org/10.1016/j.fuel.2016.11.100>.
- Kleen, M., Ohta-aho, T., Tamminen, T., 2003. On the interaction of HBT with pulp lignin during mediated laccase delignification - a study using fractionated pyrolysis-GC/MS. *J. Anal. Appl. Pyrolysis* 70, 589–600. [https://doi.org/10.1016/S0165-2370\(03\)00028-7](https://doi.org/10.1016/S0165-2370(03)00028-7).
- Krook, J., Svensson, N., Eklund, M., 2012. Landfill mining: a critical review of two decades of research. *Waste Manag* 32, 513–520. <https://doi.org/10.1016/j.wasman.2011.10.015>.
- La Nasa, J., Biale, G., Ferriani, B., Colombini, M.P., Modugno, F., 2018. A pyrolysis approach for characterizing and assessing degradation of polyurethane foam in cultural heritage objects. *J. Anal. Appl. Pyrolysis* 134, 562–572. <https://doi.org/10.1016/j.jaap.2018.08.004>.
- Laner, D., Esguerra, J.L., Krook, J., Horttanainen, M., Kriipalu, M., Rosendal, R.M., Stanislavljević, N., 2019. Systematic assessment of critical factors for the economic performance of landfill mining in Europe: what drives the economy of landfill mining? *Waste Manag* 95, 674–686. <https://doi.org/10.1016/j.wasman.2019.07.007>.
- Lehrle, R.S., Parsons, I.W., Rollinson, M., 2000. Thermal degradation mechanisms of Nylon 6 deduced from kinetic studies by pyrolysis-g. *c. Polym. Degrad. Stab.* 67, 21–33.
- Liu, J., Li, X., Xu, L., Zhang, P., 2016. Investigation of aging behavior and mechanism of nitrile-butadiene rubber (NBR) in the accelerated thermal aging environment. *Polym. Test.* 54, 59–66. <https://doi.org/10.1016/j.polymertesting.2016.06.010>.
- Lokahita, B., Samudro, G., Huboyo, H.S., Aziz, M., Takahashi, F., 2019. Energy recovery potential from excavating municipal solid waste dumpsite in Indonesia. *Energy Procedia* 158, 243–248. <https://doi.org/10.1016/j.egypro.2019.01.083>.
- Lopez, G., Artetxe, M., Amutio, M., Bilbao, J., Olazar, M., 2017. Thermochemical routes for the valorization of waste polyolefinic plastics to produce fuels and chemicals. *A review. Renew. Sustain. Energy Rev.* 73, 346–368. <https://doi.org/10.1016/j.rser.2017.01.142>.
- Mattonai, M., Licursi, D., Antonetti, C., Raspolli Galletti, A.M., Ribechini, E., 2017. Py-GC/MS and HPLC-DAD characterization of hazelnut shell and cuticle: Insights into possible re-evaluation of waste biomass. *J. Anal. Appl. Pyrolysis* 127, 321–328. <https://doi.org/10.1016/j.jaap.2017.07.019>.
- Mattonai, M., Watanabe, A., Shiono, A., Ribechini, E., 2019. Degradation of wood by UV light : a study by EGA-MS and Py-GC / MS with on line irradiation system. *J. Anal. Appl. Pyrolysis* 139, 224–232. <https://doi.org/10.1016/j.jaap.2019.02.009>.
- Miranda, R., Sosa Blanco, C., Bustos-Martinez, D., Vasile, C., 2007. Pyrolysis of textile wastes I. Kinetics and yields. *J. Anal. Appl. Pyrolysis* 80, 489–495. <https://doi.org/10.1016/j.jaap.2007.03.008>.
- Moldovan, A., Patachia, S., Buican, R., Tereanu, M.H., 2012. Characterization of polyolefins wastes by FTIR spectroscopy. *Ser. I Eng. Sci.* 5, 65–72.
- Mönkäre, T., Palmroth, M.R.T., Sormunen, K., Rintala, J., 2019. Scaling up the treatment of the fine fraction from landfill mining: Mass balance and cost structure. *Waste Manag* 87, 464–471. <https://doi.org/10.1016/j.wasman.2019.02.032>.
- Mönkäre, T.J., Palmroth, M.R.T., Rintala, J.A., 2017. Screening biological methods for laboratory scale stabilization of fine fraction from landfill mining. *Waste Manag* 60, 739–747. <https://doi.org/10.1016/j.wasman.2016.11.015>.
- Mönkäre, T.J., Palmroth, M.R.T., Rintala, J.A., 2016. Characterization of fine fraction mined from two Finnish landfills. *Waste Manag* 47, 34–39. <https://doi.org/10.1016/j.wasman.2015.02.034>.
- Nahil, M.A., Williams, P.T., 2010. Activated carbons from acrylic textile waste. *J. Anal. Appl. Pyrolysis* 89, 51–59. <https://doi.org/10.1016/j.jaap.2010.05.005>.
- Ohtani, H., Nagaya, T., Sugimura, Y., Tsuge, S., 1982. Studies on thermal degradation of aliphatic polyamides by pyrolysis-glass capillary gas chromatography. *J. Anal. Appl. Pyrolysis* 4, 117–131.
- Panda, A.K., Singh, R.K., Mishra, D.K., 2010. Thermolysis of waste plastics to liquid fuel. A suitable method for plastic waste management and manufacture of value added products-A world prospective. *Renew. Sustain. Energy Rev.* 14, 233–248. <https://doi.org/10.1016/j.rser.2009.07.005>.
- Park, S.S., Seo, D.K., Lee, S.H., Yu, T.U., Hwang, J., 2012. Study on pyrolysis characteristics of refuse plastic fuel using lab-scale tube furnace and thermogravimetric analysis reactor. *J. Anal. Appl. Pyrolysis* 97, 29–38. <https://doi.org/10.1016/j.jaap.2012.06.009>.
- Parrodi, J.C.H., Höllen, D., Pomberger, R., 2018. Characterization of fine fractions from landfill mining: a review of previous investigations. *Detritus* 2, 46–62. <https://doi.org/10.31025/2611-4135/2018.13663>.
- Parrodi, J.C.H., Vollprecht, D., Pomberger, R., 2020. Case study on enhanced landfill mining at mont-saint-Guibert landfill in Belgium: physico-chemical characterization and valorization potential of combustibles and inert fractions recovered from fine fractions. *Detritus* 1–18.
- Pesce, M., Tamai, I., Guo, D., Critto, A., Brombal, D., Wang, X., Cheng, H., Marcomini, A., 2020. Circular economy in China: translating principles into practice. *Sustain* 12, 1–31. <https://doi.org/10.3390/su12030832>.
- Prechthai, T., Padmasri, M., Visvanathan, C., 2008. Quality assessment of mined MSW from an open dumpsite for recycling potential. *Resour. Conserv. Recycl.* 53, 70–78. <https://doi.org/10.1016/j.resconrec.2008.09.002>.
- Quaghebeur, M., Laenen, B., Geysen, D., Nielsen, P., Pontikes, Y., Van Gerven, T., Spooen, J., 2013. Characterization of landfilled materials: screening of the enhanced landfill mining potential. *J. Clean. Prod.* 55, 72–83. <https://doi.org/10.1016/j.jclepro.2012.06.012>.
- Ratnasari, D.K., Yang, W., Jönsson, P.G., 2019. Kinetic study of an H-ZSM-5/Al-MCM-41 catalyst mixture and its application in lignocellulose biomass pyrolysis. *Energy Fuels* 33, 5360–5367. <https://doi.org/10.1021/acs.energyfuels.9b00866>.
- Sabatini, F., Nacci, T., Degano, I., Colombini, M.P., 2018. Investigating the composition and degradation of wool through EGA/MS and Py-GC/MS. *J. Anal. Appl. Pyrolysis* 135, 111–121. <https://doi.org/10.1016/j.jaap.2018.09.012>.
- Salaudeen, S.A., Arku, P., Dutta, A., 2018. Gasification of plastic solid waste and competitive technologies. *Plastics to Energy: Fuel, Chemicals, and Sustainability Implications*. Elsevier Inc., pp. 269–293. <https://doi.org/10.1016/B978-0-12-813140-4.00010-8>.
- Selsbo, P., Ericsson, I., Kleen, M., 1997. Characterization of sulfur in wood pulps using pyrolysis-gas chromatography with sulfur-selective detection Part 1. Fractionated pyrolysis. *J. Anal. Appl. Pyrolysis* 43, 1–14. [https://doi.org/10.1016/S0165-2370\(97\)00055-7](https://doi.org/10.1016/S0165-2370(97)00055-7).
- Sieradzka, M., Rajca, P., Zajemska, M., Mlonka-Mędrala, A., Magdziarz, A., 2020. Prediction of gaseous products from refuse derived fuel pyrolysis using chemical modelling software - Ansys Chemkin-Pro. *J. Clean. Prod.* 248 <https://doi.org/10.1016/j.jclepro.2019.119277>.
- Singh, A., Chandel, M.K., 2019. Effect of aging on waste characteristics excavated from an Indian dumpsite and its potential valorisation. *Process Saf. Environ. Prot.* <https://doi.org/10.1016/j.psep.2019.11.025>.
- Singh, R.K., Ruj, B., Sadhukhan, A.K., Gupta, P., 2020. A TG-FTIR investigation on the co-pyrolysis of the waste HDPE, PP, PS and PET under high heating conditions. *J. Energy Inst.* 93, 1020–1035. <https://doi.org/10.1016/j.joei.2019.09.003>.
- Sophonrat, N., Sandström, L., Johansson, A.C., Yang, W., 2017. Co-pyrolysis of Mixed Plastics and Cellulose: An Interaction Study by Py-GC×GC/MS. *Energy & Fuels* 31, 11078–11090. <https://doi.org/10.1021/acs.energyfuels.7b01887>.
- Sophonrat, N., Sandström, L., Svanberg, R., Han, T., Dvinskikh, S., Lousada, C.M., Yang, W., 2019. Ex situ catalytic pyrolysis of a mixture of polyvinyl chloride and cellulose using calcium oxide for HCl adsorption and catalytic reforming of the pyrolysis products. *Ind. Eng. Chem. Res.* 58, 13960–13970. <https://doi.org/10.1021/acs.iecr.9b02299>.
- Sorum, L., Gronli, M.G., Hustad, J.E., 2001. Pyrolysis characteristics and kinetics of municipal solid waste. *Fuel* 80, 1217–1227.
- Wang, W., Liang, Chang, J., min, Cai, L., ping, Shi, S.Q., 2014. Quality improvement of pyrolysis oil from waste rubber by adding sawdust. *Waste Manag* 34, 2603–2610. <https://doi.org/10.1016/j.wasman.2014.08.016>.
- Williams, P.T., Williams, E.A., 1999. Interaction of plastics in mixed-plastics pyrolysis. *Energy and Fuels* 13, 188–196. <https://doi.org/10.1021/ef980163x>.
- Wolfsberger, T., Aldrian, A., Sarc, R., Hermann, R., Höllen, D., Budischowsky, A., Zöschner, A., Ragoßnig, A., Pomberger, R., 2015. Landfill mining: Resource potential of Austrian landfills - Evaluation and quality assessment of recovered municipal solid waste by chemical analyses. *Waste Manag. Res.* 33, 962–974. <https://doi.org/10.1177/0734242X15600051>.
- Wu, T., Hu, H., Jiang, D., Du, Y., Jiang, W., Wang, H., 2013. Identification of two polyamides (PA11 and PA1012) using pyrolysis-GC/MS and MALDI-TOF MS. *Polym. Test.* 32, 426–431. <https://doi.org/10.1016/j.polymertesting.2012.12.004>.
- Ximenes, F.A., Cowie, A.L., Barlaz, M.A., 2018. The decay of engineered wood products and paper excavated from landfills in Australia. *Waste Manag* 74, 312–322. <https://doi.org/10.1016/j.wasman.2017.11.035>.
- Yousef, S., Eimontas, J., Striugas, N., Tatarians, M., Abdelnaby, M.A., Tuckute, S., Kliucininkas, L., 2019. A sustainable bioenergy conversion strategy for textile waste with self-catalysts using mini-pyrolysis plant. *Energy Convers. Manag.* 196, 688–704. <https://doi.org/10.1016/j.enconman.2019.06.050>.
- Yu, J., Sun, L., Ma, C., Qiao, Y., Yao, H., 2016. Thermal degradation of PVC: a review. *Waste Manag* 48, 300–314. <https://doi.org/10.1016/j.wasman.2015.11.041>.
- Zaini, I.N., García López, C., Pretz, T., Yang, W., Jönsson, P.G., 2019. Characterization of pyrolysis products of high-ash excavated-waste and its char gasification reactivity and kinetics under a steam atmosphere. *Waste Manag* 97, 149–163. <https://doi.org/10.1016/j.wasman.2019.08.001>.
- Zaini, I.N., Gomez-Rueda, Y., Lopez, C.G., Ratnasari, D.K., Helsen, L., Pretz, T., Jönsson, P.G., Yang, W., 2020. Production of H₂-rich syngas from excavated landfill waste through steam co-gasification with biochar. *Energy* 207. <https://doi.org/10.1016/j.energy.2020.118208>.
- Zaini, I.N., Yang, W., Jönsson, P.G., 2017. Steam gasification of solid recovered fuel char derived from landfill waste: a kinetic study. *Energy Procedia* 142, 723–729. <https://doi.org/10.1016/j.egypro.2017.12.118>.
- Zhou, C., Fang, W., Xu, W., Cao, A., Wang, R., 2014. Characteristics and the recovery potential of plastic wastes obtained from landfill mining. *J. Clean. Prod.* 80, 80–86. <https://doi.org/10.1016/j.jclepro.2014.05.083>.
- Zhu, P., Sui, S., Wang, B., Sun, K., Sun, G., 2004. A study of pyrolysis and pyrolysis products of flame-retardant cotton fabrics by DSC, TGA, and PY-GC-MS. *J. Anal. Appl. Pyrolysis* 71, 645–655. <https://doi.org/10.1016/j.jaap.2003.09.005>.